



# Estimation of Cosmic Muon-Induced Neutron Yields via Muon Spallation in Deep Underground Environments Using $(e, e'xn)$ Cross-Section Measurements of $^{181}\text{Ta}$

Yuqi Yang<sup>1,2</sup> (Ph.D. student)

Xiufeng Weng<sup>3</sup>, Yigang Yang<sup>1,2\*</sup>

<sup>1</sup>Department of Engineering Physics, Tsinghua University, Beijing, P. R. China

<sup>2</sup>Key Laboratory of Particle & Radiation Imaging, Tsinghua University, Ministry of Education, Beijing, P. R. China

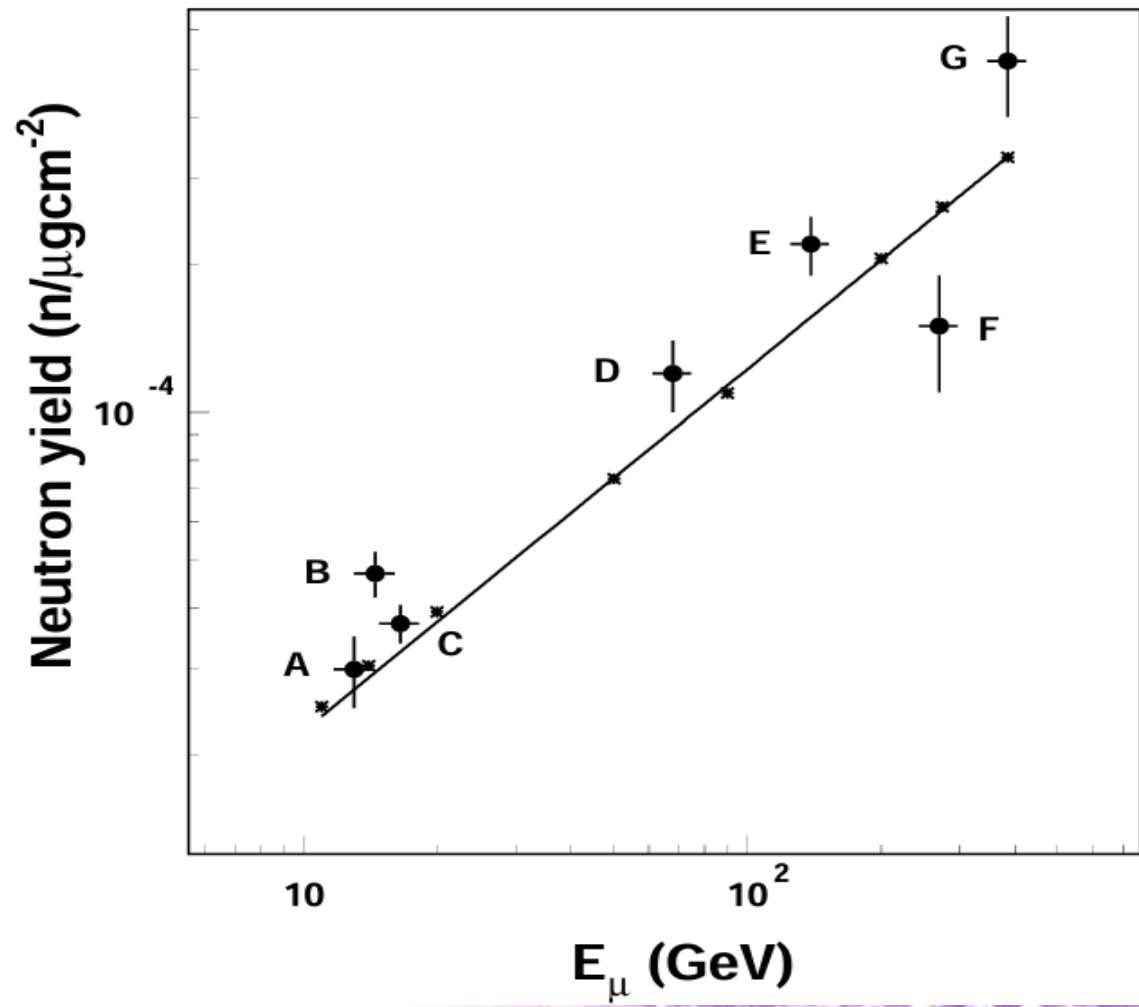
<sup>3</sup>State Key Lab. Of Intense Pulsed Radiation Simulation and Effect, Northwest Institute of Nuclear Technology, Xi'an, P. R. China

2025/05/27

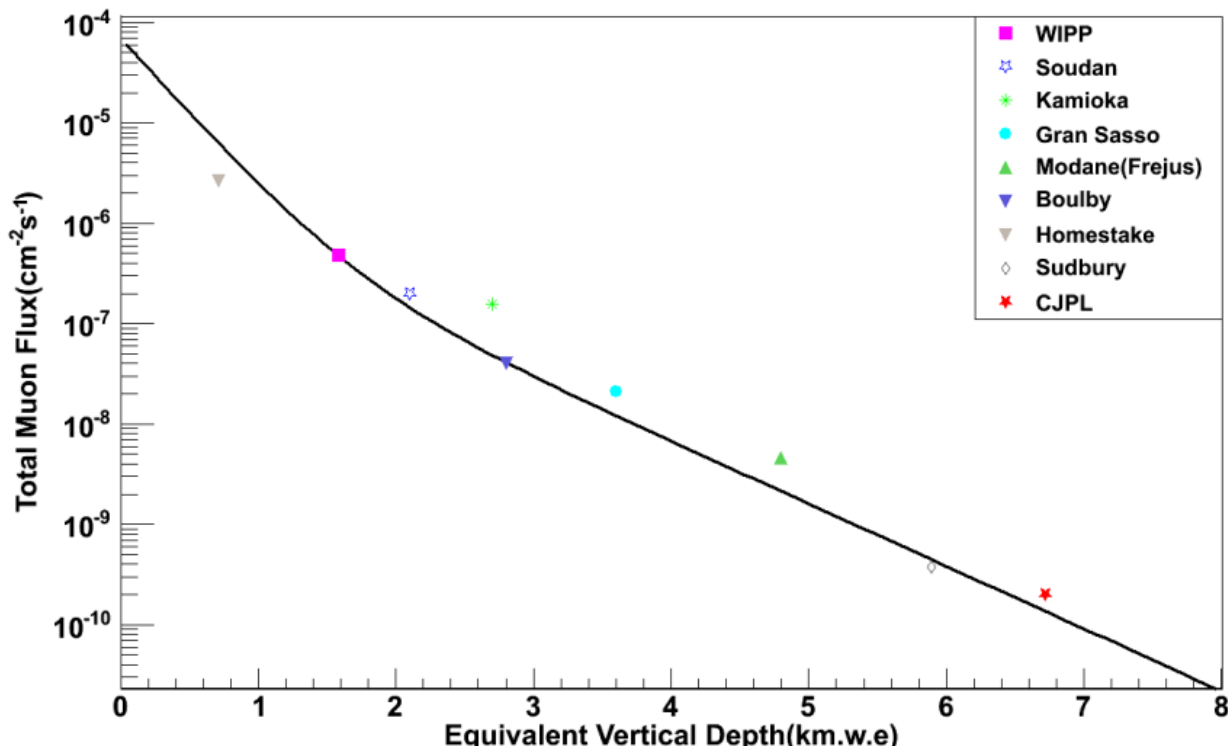
\*yangyigang@mail.Tsinghua.edu.cn

## Cosmic-muon-induced neutrons – Conflicting Data & Models

- Fast neutrons from cosmic-ray muons represent an important background for many rare-event experiments such as searches for dark matter and neutrino oscillation experiments.
- In these rare-event experiments, neutrons can mimic the target signal.
- For example, the Palo Verde reactor neutrino oscillation experiment found such neutrons to be their dominant background.
- Low-energy solar neutrino experiments such as SNO and Borexino also have to estimate such backgrounds.
- The understanding of neutron backgrounds may be relevant in resolving the controversy between the CDMS and DAMA results on dark matter searches.

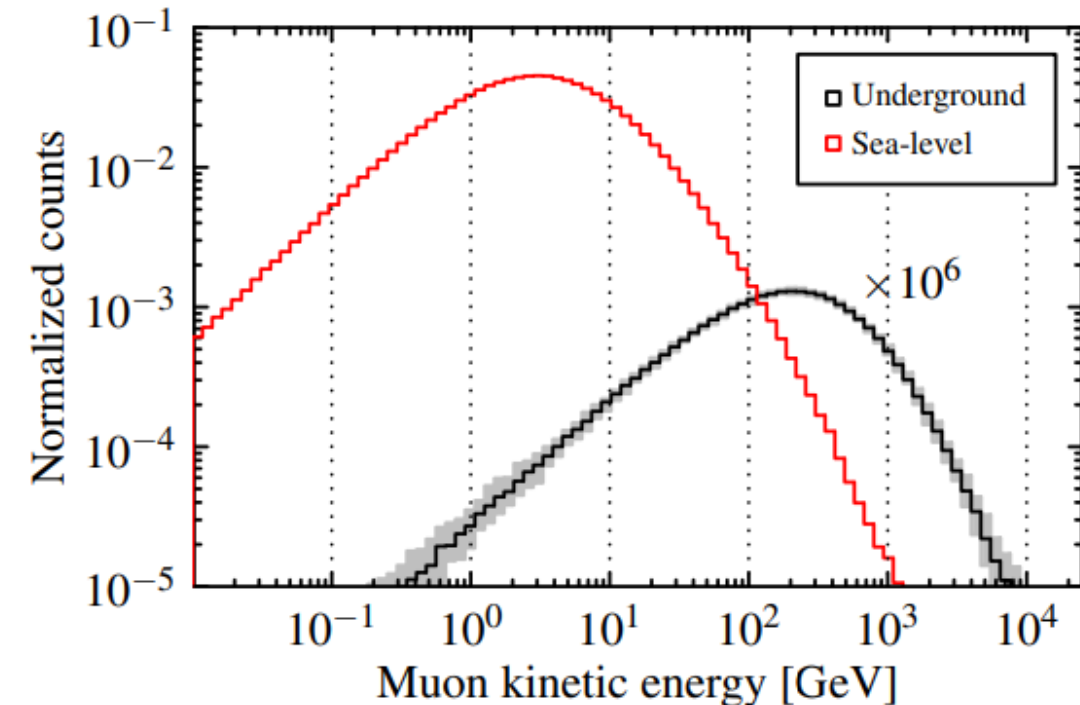


## Challenge on Measurements



Wu, Yu-Cheng, et al. *Chinese physics C* 37.8 (2013): 086001.

- CJPL (2400 m.w.e.) recorded just 343 muons in 820 days, yielding only ~8 detected neutrons.
- Due to the high energy and low flux of cosmic muons, it is challenging to directly measure the neutron yield.



Guo, Zi-yi, et al. *Chinese Physics C* 45.2 (2021): 025001.

- Black: Muon spectrum in CJPL

# Unavoidable Neutrons Produced in the Detector

Fast neutrons from cosmic-ray muons are produced in the following processes:

- a) Muon interactions with nuclei via a virtual photon producing a nuclear disintegration. This process is usually referred to as “muon spallation” and is the main source of theoretical uncertainty.
- b) Muon elastic scattering with neutrons bound in nuclei.
- c) Photo-nuclear reactions associated with electromagnetic showers generated by muons.
- d) Secondary neutron production following any of the above processes.

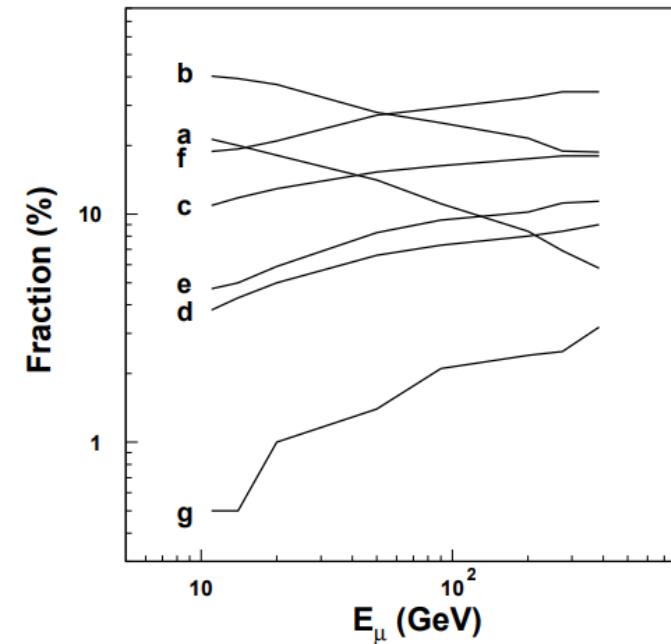
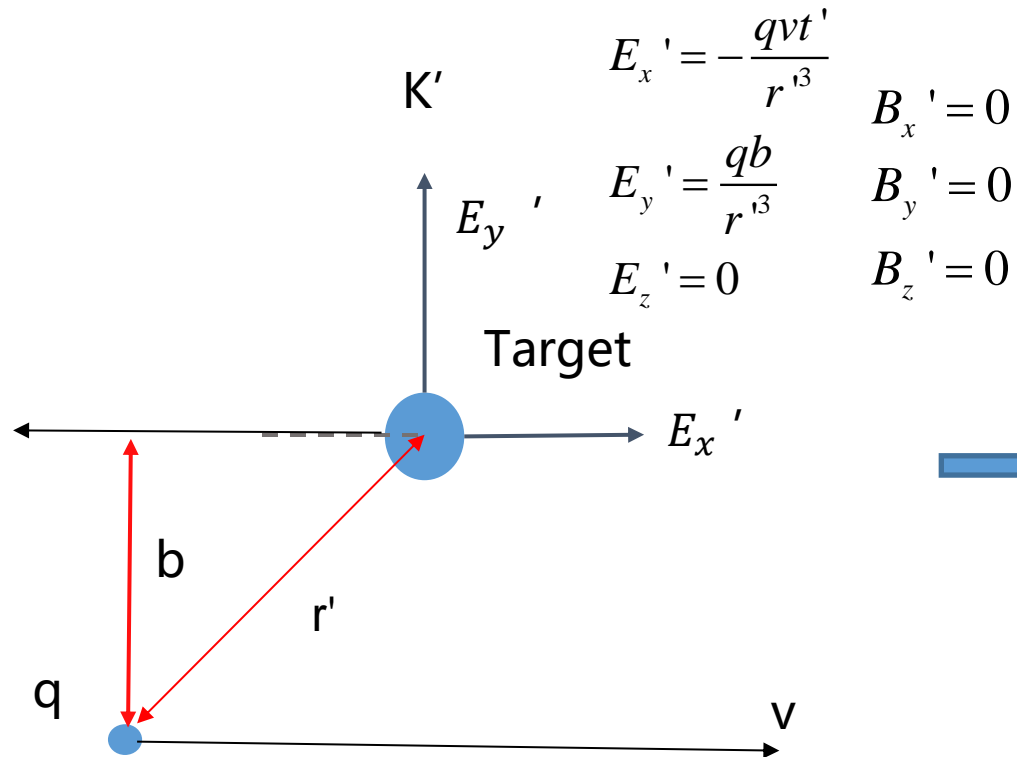


FIG. 3. Origin of neutrons: a) direct muon spallation, b) real photo-nuclear disintegration, c) neutron spallation, d) proton spallation, e)  $\pi^+$  spallation, f)  $\pi^-$  spallation and capture, g) others.

- Even if we can shield as much as possible against fast neutrons generated outside the detector, fast neutrons produced in the detector by muon spallation will always be present.
- According to the equivalent photon approximation method, the Coulomb excitation process of leptons with the same relativistic factor is similar.



## Equivalent Photon Approximation



$$E_x = E_x'$$

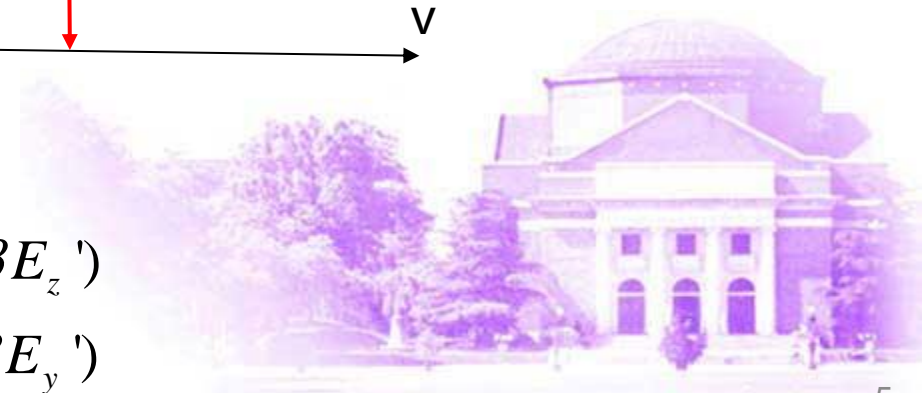
$$E_y = \gamma(E_y' + \beta B_z')$$

$$E_z = \gamma(E_z' - \beta B_y')$$

$$B_x = B_x'$$

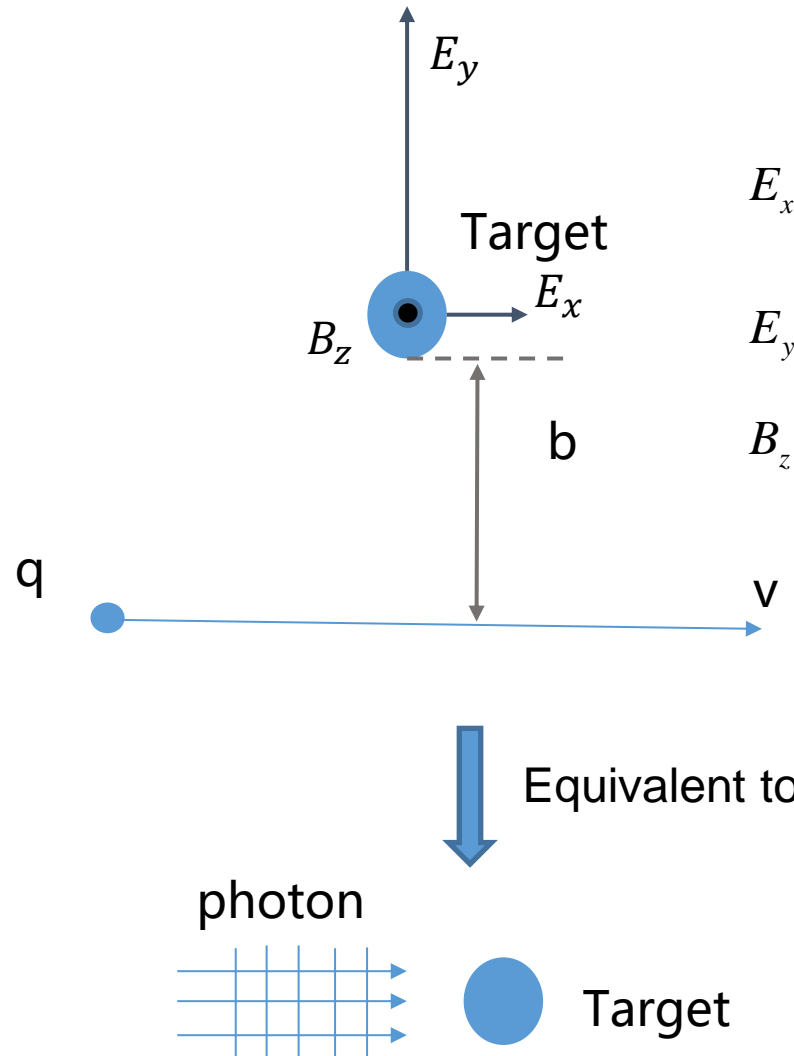
$$B_y = \gamma(B_y' - \beta E_z')$$

$$B_z = \gamma(B_z' + \beta E_y')$$





## The equivalent photon approximation



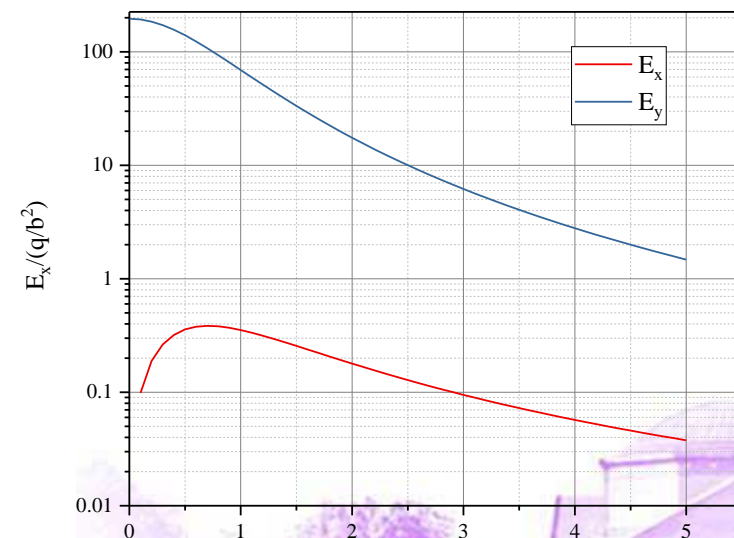
$$E_x = E_x' = -\frac{q\gamma vt}{(b^2 + \gamma^2 v^2 t^2)^{3/2}}$$

$$E_y = \gamma E_y' = \frac{q\gamma b}{(b^2 + \gamma^2 v^2 t^2)^{3/2}}$$

$$B_z = \gamma \beta E_y' = \beta E_y$$

$$\beta = \frac{v}{c} \approx 1 \Rightarrow E_y \approx B_z$$

$E_x$  and  $E_y$  when  $\gamma=200$



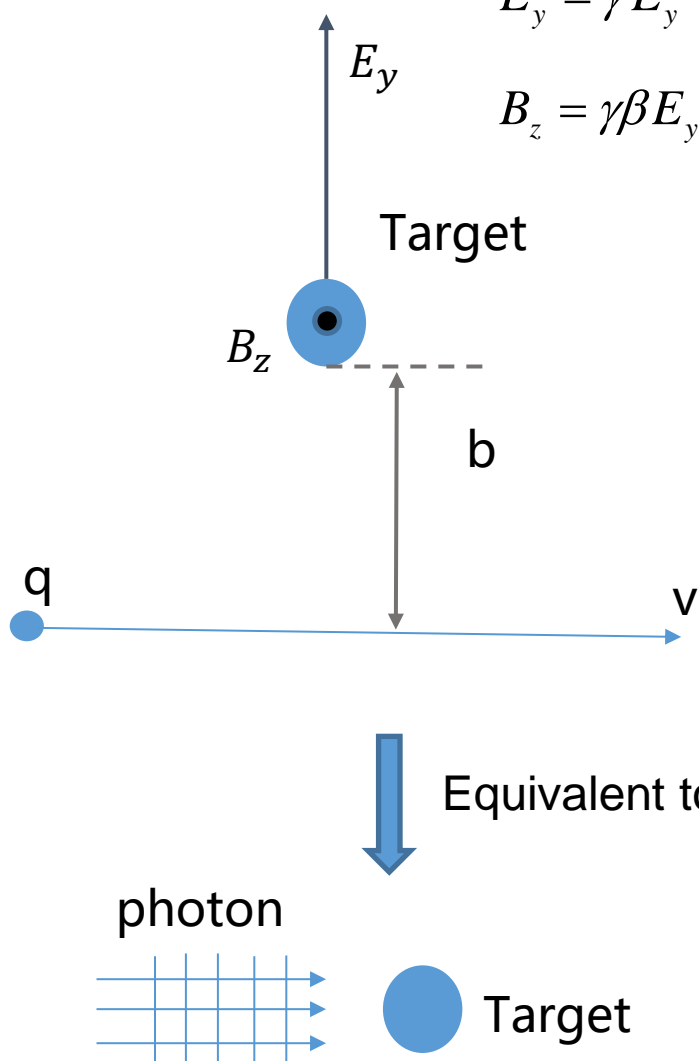
$E_x$  can be ignored

# The equivalent photon approximation

Weizsäcker-Williams method of virtual quanta:

$$E_y = \gamma E_y' = \frac{q\gamma b}{(b^2 + \gamma^2 v^2 t^2)^{3/2}}$$

$$B_z = \gamma \beta E_y' = \beta E_y$$



Fourier transform

$$\frac{d^2 I}{d\omega dA}(\omega) = c |E(\omega)|^2$$

$$\frac{d^2 I}{d\omega dA}(\omega)$$

$$\frac{dI}{d\omega}(\omega) = \int \frac{d^2 I}{d\omega dA}(\omega) 2\pi b db$$

$$\frac{dI}{d\omega}(\omega) d\omega = \hbar \omega N(\hbar\omega) d(\hbar\omega)$$

$$N(\hbar\omega) = \frac{2}{\pi} \frac{q^2}{\hbar c} \left(\frac{c}{v}\right)^2 \frac{1}{\hbar\omega} \left\{ x K_0(x) K_1(x) - \frac{v^2}{2c^2} x^2 \times [K_1^2(x) - K_0^2(x)] \right\}$$

$K_n(x)$ : Modified Bessel function of the second kind

Same impact parameter

Same Lorentz factor

Low energy transfer

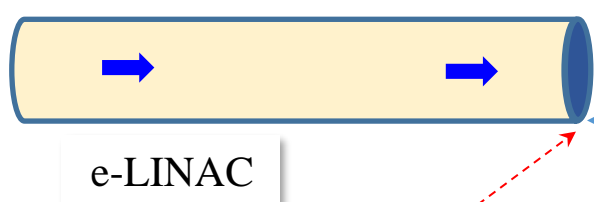
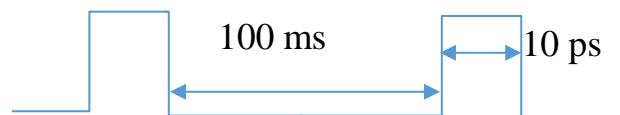
$$N(E_{e^-}) = N(E_{\mu^-}) = \frac{m_{\mu^-}}{m_{e^-}} E_{e^-} \approx 207 E_{e^-}$$

$$E_{e^-} = 100 \text{ MeV} \Leftrightarrow E_{\mu^-} = 20.7 \text{ GeV} (\text{example})$$

# Experimental process

(1)  $10\mu\text{m}$ - $^{181}\text{Ta}$  foil irradiated by electrons

electron pulses



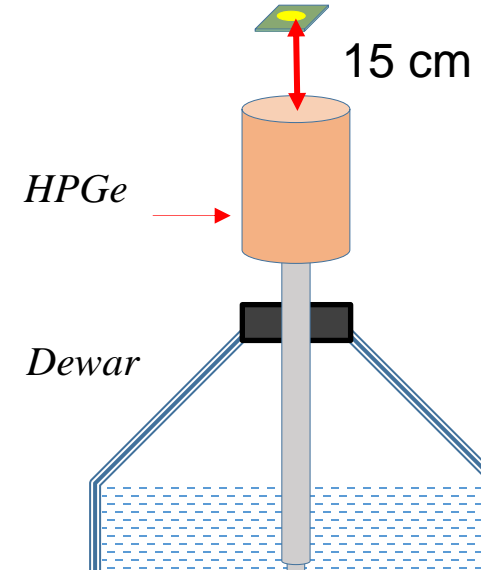
The 120 MeV Electron Linac  
at the State Key Laboratory  
of Intense Pulsed Radiation  
Simulation and Effect

Energy: 20~110 MeV  
Irradiation time: 1 h

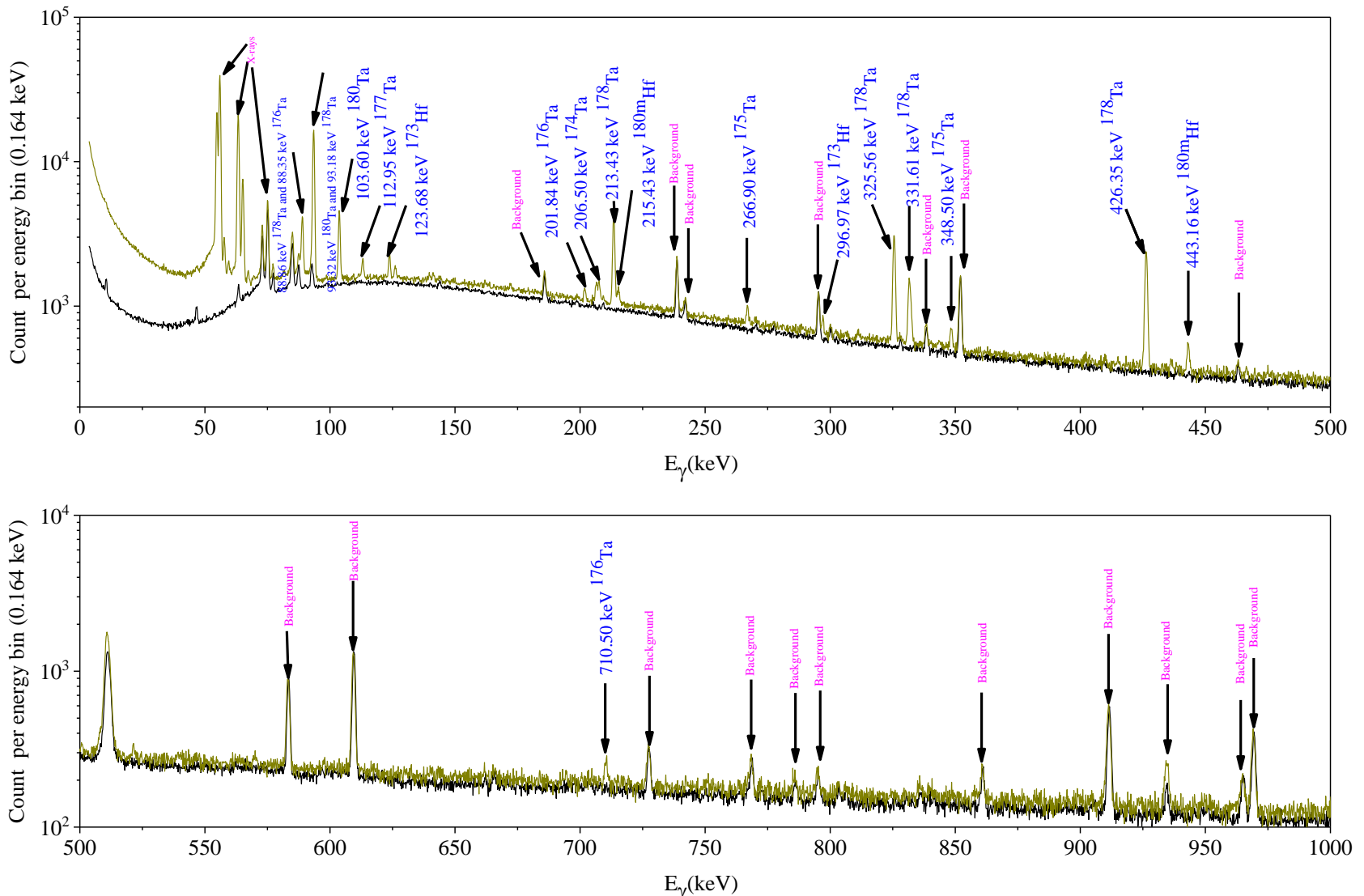
(2) : residual activity of the  $10\mu\text{m}$ - $^{181}\text{Ta}$  foil measured by a HPGe detector

Lead

Measurement time: 24 h  
Irradiated  $10\mu\text{m}$ - $^{181}\text{Ta}$  foil



# Spectrum



Yellow line: residual  $\gamma$ -activity spectrum  
Black line: background

# Calculation of measured cross sections

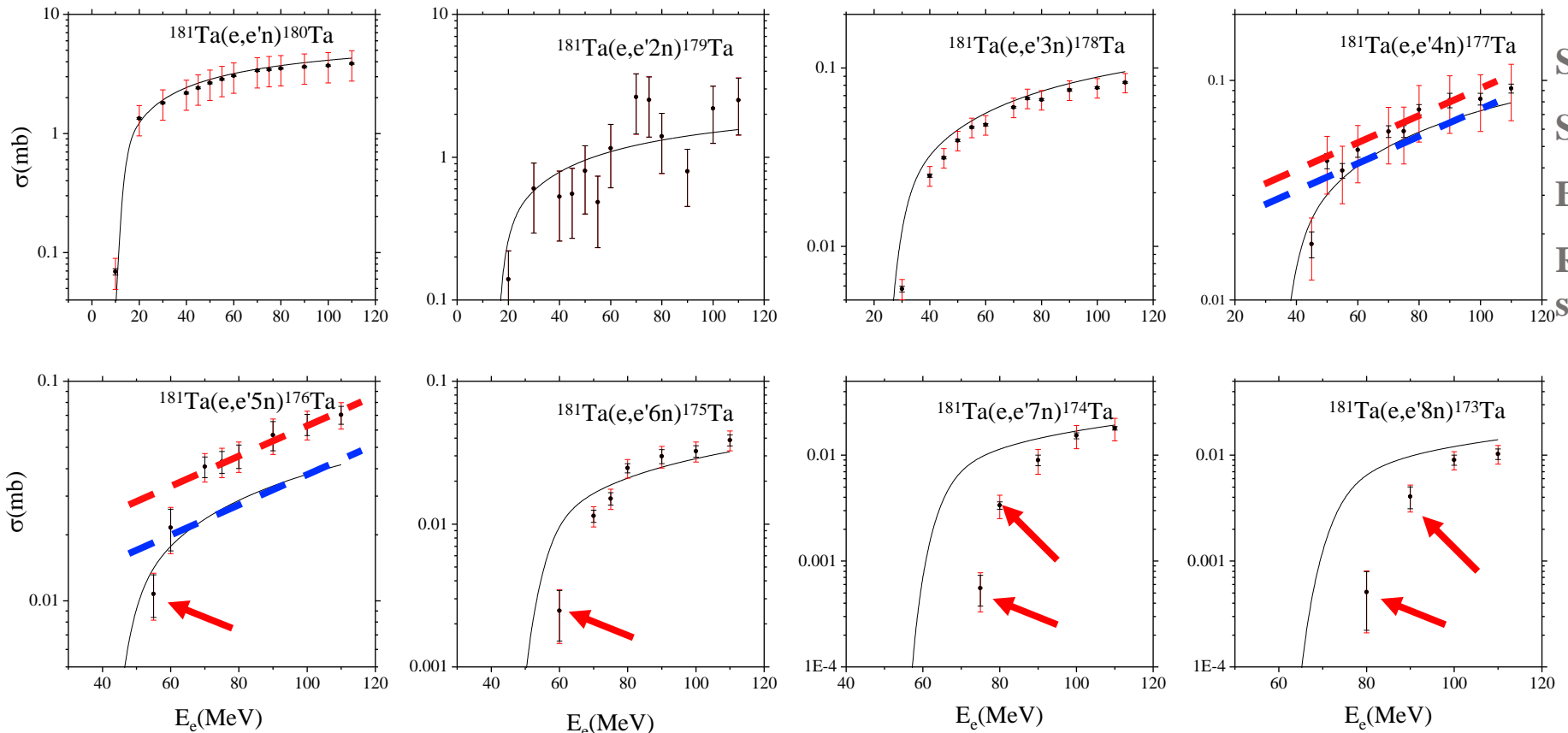
---

$$\sigma_{(e,e'xn)}^{\text{exp}} = -\frac{1}{ND} \ln \left[ 1 - \frac{N_{\text{meas}}}{N_e I_\gamma \epsilon (1 - e^{-\lambda t_{\text{irr}}}) e^{-\lambda t_{\text{cool}}} (1 - e^{-\lambda t_{\text{meas}}})} \right]$$

Symbol	Meaning	Error
$N_{\text{meas}}$	Counts of full-energy peaks	1% ~ 10%
$N_e$	Number of bombarding electrons	2.5%
$\epsilon$	Absolute detection efficiency for full-energy peaks of gamma-rays	2%
$I_\gamma$	Intensity of emitted gamma-ray for each decay of $^{181-x}\text{Ta}$	1 ~ 20%
$\lambda$	Decay constant of $^{181-x}\text{Ta}$	0.1% ~ 7%
$t_{\text{irr}}, t_{\text{cool}}, t_{\text{meas}}$	Irradiation, cooling and measurement times	/
$N$	$^{181}\text{Ta}$ nuclei's number density	/
$D$	Thickness of tantalum foil	/

} IAEA

# Measurement result



Solid line: simulated cross-section  
 Solid circles: measured cross-section  
 Black error bars: statistical errors  
 Red error bars: total errors (both statistical and systematic errors).

- When the number of escaping neutrons reaches 5–8, a significant difference arises between the experimental and theoretical cross sections, especially when electron energies are close to threshold.
- These differences not only cast our doubt on the accuracy of the TALYS results but also highlight the potential of our approach to correct the simulation outcomes.

# Energy Dependence of Neutron Yield

Weizsäcker-Williams method of virtual quanta

$$N(\hbar\omega) = \frac{2}{\pi} \frac{q^2}{\hbar c} \left(\frac{c}{v}\right)^2 \frac{1}{\hbar\omega} \left\{ x K_0(x) K_1(x) - \frac{v^2}{2c^2} x^2 \times [K_1^2(x) - K_0^2(x)] \right\}$$
$$\xrightarrow{\hbar\omega \ll E_e} N(\hbar\omega) = \frac{2e^2}{\pi c \hbar^2 \omega} \left[ \ln\left(\frac{1.123\gamma c}{\omega b_{\min}}\right) - \frac{1}{2} \right]$$

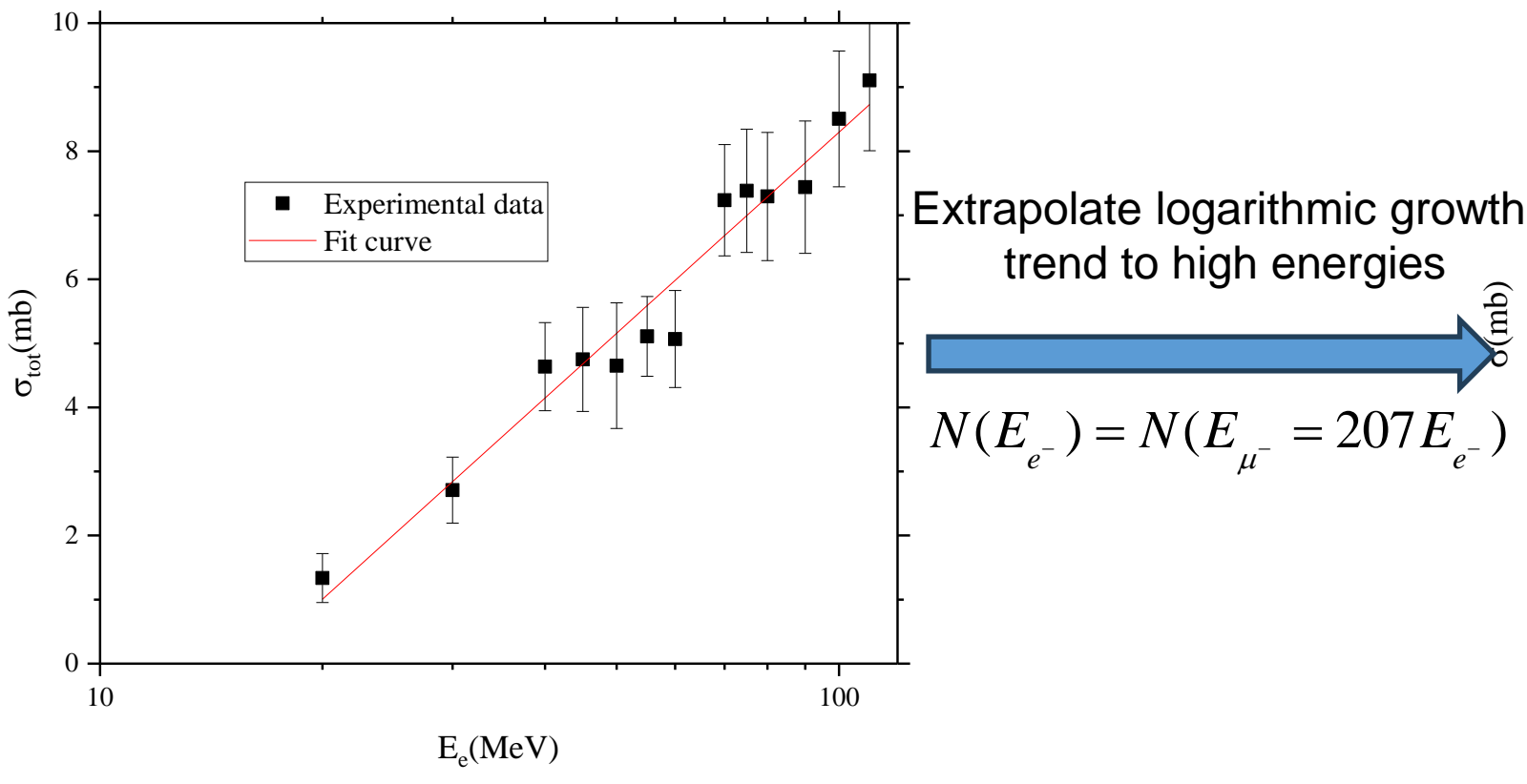
$$\begin{aligned}\sigma_{(e,e'xn)}(E_e) &= \int_{E_{th}}^{E_e} \sigma_{(\gamma,xn)}(E_\gamma) N_{virtual}(E_\gamma, E_e) dE_\gamma \\ &= \int_{E_{th}}^{E_e} \sigma_{(\gamma,xn)}(E_\gamma) \frac{2e^2}{\pi c \hbar^2 \omega} \left[ \ln(E_e) + \ln\left(\frac{1.123c}{0.511\omega b_{\min}}\right) - \frac{1}{2} \right] dE_\gamma \\ &= \int_{E_{th}}^{E_e} \sigma_{(\gamma,xn)}(E_\gamma) \frac{2e^2}{\pi c \hbar^2 \omega} dE_\gamma \ln(E_e) + \int_{E_{th}}^{E_e} \sigma_{(\gamma,xn)}(E_\gamma) \frac{2e^2}{\pi c \hbar^2 \omega} \left[ \ln\left(\frac{1.123c}{0.511\omega b_{\min}}\right) - \frac{1}{2} \right] dE_\gamma \\ &= A \cdot \ln(E_e) + B\end{aligned}$$



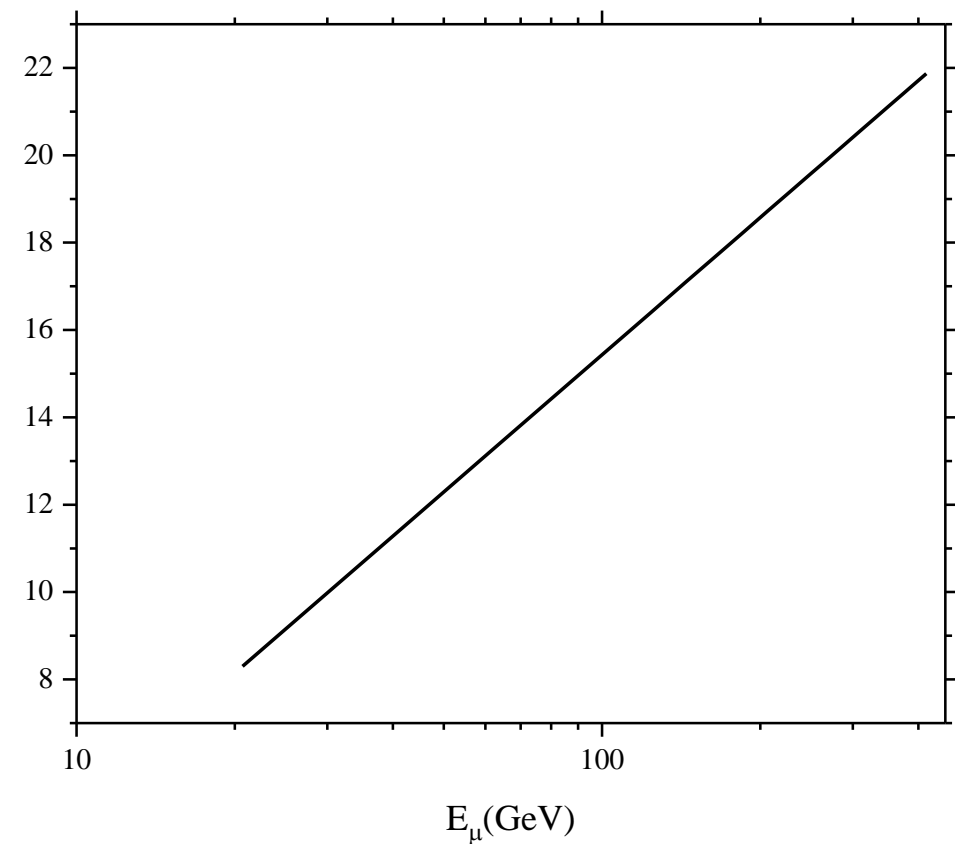
For electrons with energies far above the energy at the peak of the cross-section, the trend of the Coulomb excitation cross-section should be a **logarithmic increase** as the electron energy increases.

# Energy Dependence of Neutron Yield

Electron-induced-neutron-production cross section  
vs Electron energy



Muon-induced-neutron-production cross section  
vs Muon energy



# Nuclear Dependence of Neutron Yield

- Assume the neutron-production cross section is dominated by the GDR contribution

- GDR sum rule::

$$\int \sigma_\gamma(E_\gamma) dE_\gamma = \frac{2\pi^2 e^2 \hbar}{Mc} \cdot \frac{NZ}{A}$$

- GDR resonance energy vs. mass number A:

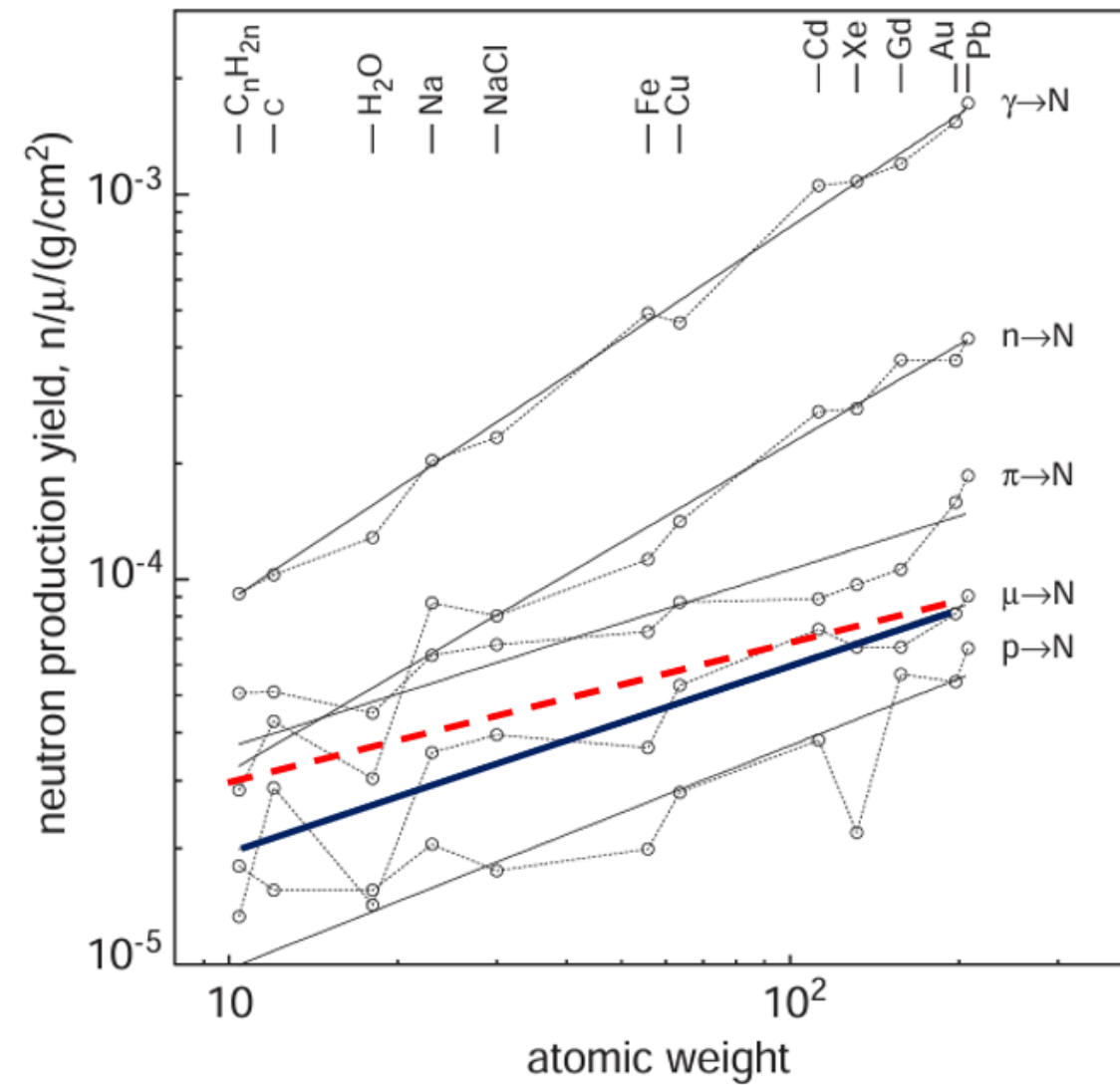
$$E_r = 31.2A^{-1/3} + 20.6A^{-1/6}$$

- Virtual photon spectrum vs. photon energy:

$$N(\hbar\omega) = \frac{2e^2}{\pi c \hbar^2 \omega} \left[ \ln\left(\frac{1.123\gamma c}{\omega b_{\min}}\right) - \frac{1}{2} \right]$$

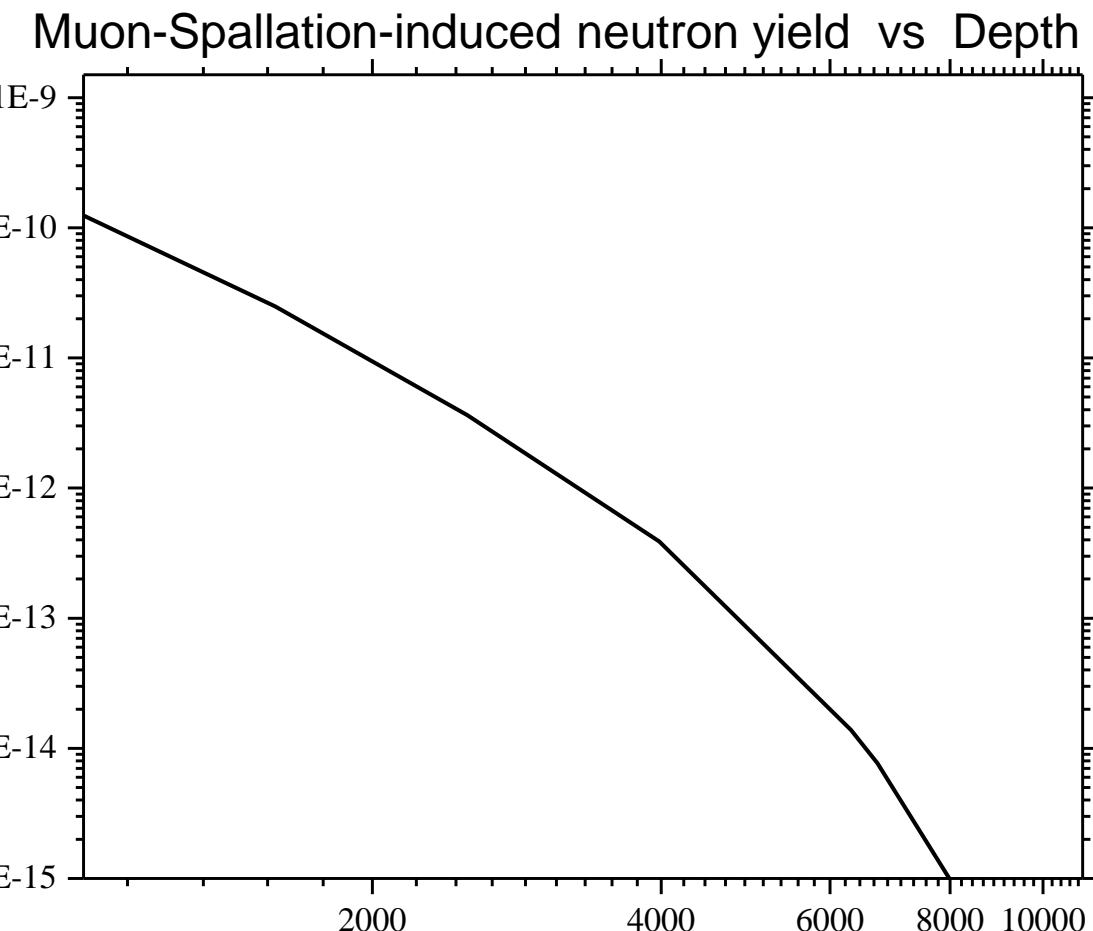
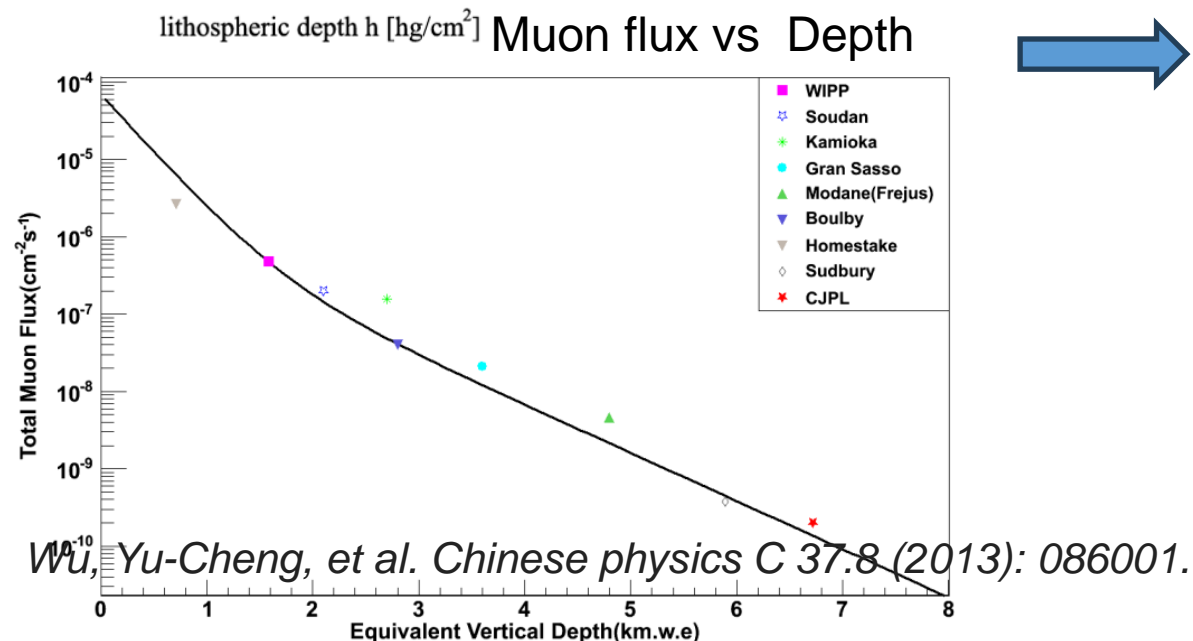
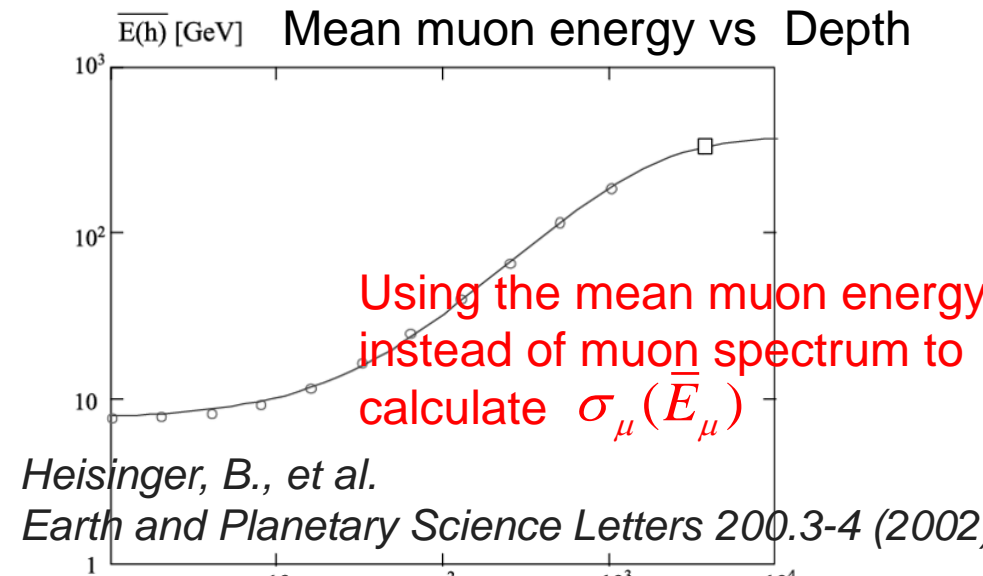
- Assume Virtual photon spectrum varies slowly across the GDR region, then

$$\begin{aligned} \sigma_\mu(E_\mu) &= \int N_{\text{virtual}}(E_\gamma, E_\mu) \sigma_\gamma(E_\gamma) dE_\gamma \\ &= N_{\text{virtual}}(E_r, E_\mu) \int \sigma_\gamma(E_\gamma) dE_\gamma \underset{\text{red circle}}{\approx} \frac{NZ}{A} \cdot \frac{A - B \ln E_r}{E_r} \end{aligned}$$



[1] Araujo, H. M., et al. Nuclear Instruments and Methods in Physics Research Section A: Accelerators, Spectrometers, Detectors and Associated Equipment 545.1-2 (2005): 398-411.

# Depth Dependence of Neutron Yield



Serving as a lower limit for the neutron background in deep-underground measurements



## Conclusion

---

- According to the Weizsäcker-Williams virtual photon method, the Coulomb excitation process of leptons with the same relativistic factor is similar.
- Based on this, we propose a method to estimate the neutron yield induced by cosmic-ray muons via Coulomb excitation in detectors by measuring the neutron yield from electron Coulomb excitation, thereby providing a lower-bound estimate of the neutron background in deep-underground measurements.
- More measurements of electron-induced neutron yields for each target material are needed for more accurate evaluation of nuclear dependence of the neutron yield induced by cosmic-ray muons via Coulomb excitation.





THANK YOU FOR LISTENING!

